

## Stardust in Antarctic micrometeorites

Toru YADA<sup>1,2</sup>, Christine FLOSS<sup>1\*</sup>, Frank J. STADERMANN<sup>1</sup>, Ernst ZINNER<sup>1</sup>,  
Tomoki NAKAMURA<sup>3</sup>, Takaaki NOGUCHI<sup>4</sup>, and A. Scott LEA<sup>5</sup>

<sup>1</sup>Laboratory for Space Sciences and Physics Department, CB 1105, Washington University, Saint Louis, Missouri 63130, USA

<sup>2</sup>Japan Aerospace Exploration Agency, Institute of Space and Astronautical Science, Sagami-hara, Kanagawa 229–8510, Japan

<sup>3</sup>Department of Earth and Planetary Science, Graduate School of Science, Kyushu University, Hakozaki, Fukuoka 812–8581, Japan

<sup>4</sup>Department of Materialogical and Biological Sciences, Ibaraki University, Mito, Ibaraki 310–8512, Japan

<sup>5</sup>Pacific Northwest National Laboratory, P.O. Box 999, Richland, Washington 99352, USA

Corresponding author. E-mail: [floss@wustl.edu](mailto:floss@wustl.edu)

(Received 28 June 2007; revision accepted 07 March 2008)

---

**Abstract**—We report the discovery of presolar silicate, oxide (hibonite), and (possibly) SiC grains in four Antarctic micrometeorites (AMMs). The oxygen isotopic compositions of the eighteen presolar silicate (and one oxide) grains found are similar those observed previously in primitive meteorites and interplanetary dust particles, and indicate origins in oxygen-rich red giant or asymptotic giant branch stars, or in supernovae. Four grains with anomalous C isotopic compositions were also detected. <sup>12</sup>C/<sup>13</sup>C as well as Si ratios are similar to those of mainstream SiC grains; the N isotopic composition of one grain is also consistent with a mainstream SiC classification.

Presolar silicate grains were found in three of the seven AMMs studied, and are heterogeneously distributed within these micrometeorites. Fourteen of the 18 presolar silicate grains and 3 of the 4 C-anomalous grains were found within one AMM, T98G8. Presolar silicate-bearing micrometeorites contain crystalline silicates that give sharp X-ray diffractions and do not contain magnesiowüstite, which forms mainly through the decomposition of phyllosilicates and carbonates. The occurrence of this mineral in AMMs without presolar silicates suggests that secondary parent body processes probably determine the presence or absence of presolar silicates in Antarctic micrometeorites.

---

### INTRODUCTION

Since the first separation of presolar diamonds and SiC grains from carbonaceous chondrites, presolar graphite, Si<sub>3</sub>N<sub>4</sub>, oxides, silicates and various carbides have been identified in primitive meteorites on the basis of their C, N, O and Si isotopic ratios, which are distinct from those of solar system materials (e.g., Zinner 2004). The discovery of presolar silicates in both anhydrous interplanetary dust particles (IDPs; Messenger et al. 2003) and carbonaceous chondrites (Nguyen and Zinner 2004; Nagashima et al. 2004) confirmed astronomical observations indicating the presence of crystalline and amorphous silicates in circumstellar environments (e.g., Waters et al. 1996; Demyk et al. 2000). Moreover, presolar silicates are apparently more abundant in primitive extraterrestrial materials than other types of presolar grains (Floss et al. 2006; Nguyen et al. 2007). The abundances of different types of presolar grains in extraterrestrial samples can provide information not only about the degree of aqueous and thermal alteration experienced by a given parent body but

also about the abundance of presolar grains in the accretion region of that parent body in the early solar nebula.

Micrometeorites are extraterrestrial dust particles with sizes up to several hundred micrometers in diameter that are collected in the polar regions of the Earth (e.g., Maurette et al. 1986, 1991; Yada and Kojima 2000). They are thought to come from both asteroids and comets, although mineralogical and chemical studies show that they are similar to carbonaceous chondrites, suggesting that most originated from asteroids (Kurat et al. 1994; Nakamura et al. 2001; Noguchi et al. 2002). Although micrometeorites dominate the flux of all extraterrestrial materials on Earth (Love and Brownlee 1993; Taylor et al. 1998; Yada et al. 2004) and presolar components have long been predicted (Maurette 2006), previous searches for presolar grains in these particles were unsuccessful (Prombo et al. 1991; Yates 1993; Strebel et al. 1998). Here, we report on the discovery of presolar grains in Antarctic micrometeorites (AMMs). Preliminary results have been reported by Yada et al. (2005a, 2005b, 2006).

## EXPERIMENTAL

The AMMs analyzed in this study were obtained from particles collected by filtering melted blue ice at Tottuki Point, 17 km northeast of Syowa Station, in East Antarctica (Yada and Kojima 2000; Iwata and Imae 2002). Candidate micrometeorites were handpicked from the 100–238  $\mu\text{m}$  size fraction under a stereomicroscope, and were measured with the JEOL JSM5300LV scanning electron microscope equipped with an energy dispersive X-ray spectrometer (SEM-EDX) at Ibaraki University and the JEOL JSM5800LV SEM-EDX at Kyushu University to obtain backscattered electron (BSE) images of their surfaces and EDX spectra for qualitative chemical analyses. In total, 85 particles were identified as AMMs based on their chondritic chemical compositions. In order to investigate their bulk mineralogies, individual AMMs were exposed to synchrotron X-rays with a wavelength of  $2.161 \pm 0.001 \text{ \AA}$  in a Gandolfi camera to obtain X-ray diffraction patterns. The X-ray diffraction (XRD) analysis was performed at beamline 4A of the Photon Factory Institute of Material Science, High Energy Accelerator Research Organization, located in Tsukuba, Japan. The ultra-high-intensity monochromatic X-rays allowed us to obtain clear X-ray powder diffraction patterns from the AMMs within a short exposure time of approximately 30 minutes. The XRD procedures are described in detail by Nakamura et al. (2001). Fine-grained AMMs that were not severely heated were selected for isotopic measurements. Coarse-grained AMMs, which are more likely to have undergone igneous processing and scoriaceous AMMs, which experienced severe heating during atmospheric entry were specifically avoided for this study, as these were deemed less likely to contain surviving presolar grains. The selected AMMs (T98NF2, -H3, -H5, -G6, -G8 and T00Iba030) were then pressed into high purity Au foil for isotopic characterization in the Washington University NanoSIMS. One C-rich AMM, TT54B397, mounted in epoxy resin and polished to expose its cross-section was also analyzed in the NanoSIMS.

The NanoSIMS measurements followed standard procedures (Stadermann et al. 2005; Floss et al. 2006): an  $\sim 1 \text{ pA}$   $\text{Cs}^+$  primary ion beam, with a diameter of  $\sim 100 \text{ nm}$ , was rastered over small areas on the samples, and negative secondary ions were sent through a double-focusing mass spectrometer and were detected in a multi-collector system of electron multipliers. Most measurements consisted of multiple  $512^2$  pixel scans over  $20 \times 20 \mu\text{m}^2$  areas, during which ions of  $^{12}\text{C}^-$ ,  $^{13}\text{C}^-$ ,  $^{16}\text{O}^-$ ,  $^{17}\text{O}^-$  and  $^{18}\text{O}^-$ , as well as secondary electrons (SE) were collected simultaneously. A single analysis typically lasted more than six hours. Isotopic ratios were normalized to the average isotopic composition of each Antarctic micrometeorite and grains were considered anomalous if their isotopic compositions deviated by more than  $3\sigma$  from the range of normal sub-grains within a given

micrometeorite. Enhancements in  $^{17}\text{O}/^{16}\text{O}$  and  $^{18}\text{O}/^{16}\text{O}$  can, in principle, arise from the quasi-simultaneous arrival (QSA) of two  $^{16}\text{O}$  ions on a detector, that are counted as a single ion (Slodzian et al. 2004), as a result of the high transmission and high sensitivity of O in the NanoSIMS. The grains found in this study were examined individually to ensure that this effect is not responsible for the observed anomalies. For grains with isotopically anomalous oxygen or carbon, we subsequently analyzed the Si isotopes: ( $^{16}\text{O}^-$ ,  $^{17}\text{O}^-$  or  $^{18}\text{O}^-$ ) or ( $^{12}\text{C}^-$ ,  $^{13}\text{C}^-$ ),  $^{28}\text{Si}^-$ ,  $^{29}\text{Si}^-$ ,  $^{30}\text{Si}^-$ . One grain was also analyzed for N isotopes:  $^{12}\text{C}^-$ ,  $^{13}\text{C}^-$ ,  $^{12}\text{C}^{14}\text{N}^-$ ,  $^{12}\text{C}^{15}\text{N}^-$ ,  $^{28}\text{Si}^-$ .

Grains identified as presolar by NanoSIMS analysis were characterized in a field-emission (FE) SEM, and elemental compositions were determined from energy dispersive X-ray (EDX) spectra obtained with 10 kV accelerating voltage and 5 nA beam current. Several presolar grains were further characterized with the PHI 680 Scanning Auger Microprobe at Pacific Northwest National Laboratory (PNNL), using a 10 kV 10 nA primary electron beam with a diameter of  $\sim 20 \text{ nm}$ . Collected spectra were subjected to 9 point smoothing and a 5 point differentiation Savitsky-Golay routine prior to peak identification.

## RESULTS

### Presolar Grains

We analyzed a total area of  $36,600 \mu\text{m}^2$  in the seven AMMs and found 19 grains with anomalous O isotopic compositions and 4 grains with anomalous C isotopic compositions. Table 1 lists the sizes and isotopic compositions of these presolar grains. Two presolar grains were found in TT54B397, three in T98H5, 17 in T98G8 and one was found in T00Iba030. Figure 1 shows the oxygen isotopic compositions of 18 of the 19 O-anomalous grains. Eleven of the grains exhibit enrichments in  $^{17}\text{O}$ , with solar to sub-solar  $^{18}\text{O}/^{16}\text{O}$  ratios, and may be classified as group 1 grains (Nittler et al. 1997). The other seven grains are enriched in  $^{18}\text{O}$ , either with or without modest  $^{17}\text{O}$  enrichments, similar to the group 4 oxide grains of Nittler et al. (1997). The final grain, T98G8-21P2, was discovered during Si isotopic analysis of adjacent anomalous grains (during which  $^{16}\text{O}$  and  $^{17}\text{O}$  were also monitored) and thus only its  $^{17}\text{O}/^{16}\text{O}$  ratio is known. This grain is enriched in  $^{17}\text{O}$  and is likely to be a group 1 grain (Table 1). Figure 2 shows the Si isotopic compositions of most of the O-anomalous grains. Most compositions are consistent with solar within  $3\sigma$  (or less) errors (Table 1). However, grain T98H5-4P1 is enriched in  $^{29}\text{Si}$  and its composition differs from solar by more than  $4\sigma$  (Table 1); it lies close to the correlation line for mainstream SiC grains (Fig. 2).

The O-anomalous grains range in size from about 200 to 600 nm (Table 1), and EDX analyses indicate that all but one of them are silicates. The excitation volume at a given beam energy during EDX analyses tends to decrease with

Table 1. Presolar grains in Antarctic micrometeorites.<sup>1</sup>

Grain	Size (nm)	Group	<sup>17</sup> O/ <sup>16</sup> O (× 10 <sup>-4</sup> )	<sup>18</sup> O/ <sup>16</sup> O (× 10 <sup>-3</sup> )	<sup>12</sup> C/ <sup>13</sup> C	<sup>14</sup> N/ <sup>15</sup> N	δ <sup>29</sup> Si (‰)	δ <sup>30</sup> Si (‰)
TT54B397-2P1	550 × 550	4	5.98 ± 0.43	3.01 ± 0.09			-33 ± 27	-34 ± 34
TT54B397-2P2	400 × 200	4	4.72 ± 0.55	2.93 ± 0.13			-46 ± 72	143 ± 98
T98H5-1P1	300 × 200	1	13.9 ± 1.2	1.90 ± 0.13			18 ± 85	68 ± 108
T98H5-4P1	600 × 600	1	8.80 ± 0.23	1.42 ± 0.03			111 ± 27	47 ± 32
T98H5-15P1	500 × 400	1	8.57 ± 0.60	2.05 ± 0.09			31 ± 61	19 ± 75
T98G8-4P1	500 × 400	4	3.44 ± 0.19	2.76 ± 0.05			16 ± 65	12 ± 76
T98G8-8P1	400 × 400	4	4.28 ± 0.55	4.87 ± 0.18			0 ± 42	58 ± 52
T98G8-12P1	300 × 250	4	3.65 ± 0.35	2.75 ± 0.09			82 ± 86	-87 ± 93
T98G8-20P1	600 × 300	1	7.00 ± 0.44	1.68 ± 0.07				
T98G8-21P1	350 × 350	1	19.5 ± 0.6	1.99 ± 0.07			18 ± 44	-23 ± 53
T98G8-21P2	200 × 200	1	12.5 ± 0.5				211 ± 90	-58 ± 97
T98G8-21P3	200 × 200	1	8.45 ± 0.55	1.86 ± 0.08			-54 ± 67	-140 ± 78
T98G8-21P4	400 × 200	1	9.84 ± 0.50	1.91 ± 0.07			23 ± 50	-63 ± 59
T98G8-21P5	200 × 200	1	9.80 ± 0.77	1.96 ± 0.11				
T98G8-21P6	400 × 400	1	16.2 ± 0.7	1.99 ± 0.08			-76 ± 45	-37 ± 57
T98G8-21P7	400 × 300	4	5.38 ± 0.45	3.17 ± 0.11			62 ± 26	43 ± 31
T98G8-21P8	500 × 300	4	4.35 ± 0.38	3.10 ± 0.10			29 ± 51	-26 ± 61
T98G8-21P11	300 × 300	1	14.0 ± 0.5	1.80 ± 0.06			69 ± 58	46 ± 71
T98G8-22P1	400 × 200	1	6.96 ± 0.43	1.90 ± 0.07			-16 ± 38	24 ± 47
T00IBa030-10P1	400 × 300				22.5 ± 1.6	229 ± 40	-5 ± 24	-6 ± 26
T98G8-7P1	500 × 400				51.4 ± 2.7			
T98G8-21P9	350 × 200				19.8 ± 0.9		42 ± 31	12 ± 38
T98G8-21P10	350 × 300				31.3 ± 1.1		79 ± 52	-73 ± 59

<sup>1</sup>Errors are 1σ.

increasing atomic number, but at an accelerating voltage of 10kV is likely to be larger than the sizes of the presolar grains studied here for the major silicate-forming elements. Thus, some fraction of the signal in the EDX spectra probably comes from outside of the grains we are analyzing. Nevertheless, we expect that the bulk of the signal originates from within the grain of interest and, thus, can provide some diagnostic information. In particular, we note that the EDX spectrum of T98H5-4P1 resembles that of Ca-rich pyroxene (Fig. 3) and grain T98G8-20P1 has an EDX spectrum consistent with hibonite (Fig. 4). Note, moreover, that the low Fe, Mg and Si peaks in this spectrum indicate little contribution from surrounding material, which is likely to be dominated by ferromagnesian silicates. Three of the silicates were also investigated by Auger spectroscopy; the data are qualitatively consistent with the EDX spectra for these grains and indicate that two of them (TT54B397-2P1 and -2P2) are ferromagnesian silicates with sub-equal amounts of Fe and Mg, whereas T98H5-1P1 is an Fe-rich silicate.

The four grains with anomalous C isotopic compositions range in size from about 300 to 500 nm and all exhibit enrichments in <sup>13</sup>C, with <sup>12</sup>C/<sup>13</sup>C ratios ranging from ~20 to 50. Nitrogen isotopes were also measured in grain T00IBa030-10P1; its C and N isotopic compositions (<sup>12</sup>C/<sup>13</sup>C = 22.5 ± 1.6; <sup>14</sup>N/<sup>15</sup>N = 229 ± 40; Table 1) are within the range of mainstream SiC grains (e.g., Zinner 2004). The Auger

analysis of this grain showed the presence of Si as well as a clear C enrichment in the region of this grain, although some O, Mg, and Fe were also detected. Silicon isotopic data on three of the grains (T00IBa030-10P1; T98G8-21P9, T98G8-21P10) are consistent with solar (Fig. 2).

### Antarctic Micrometeorite Bulk Mineralogies

Figure 5 shows the X-ray diffraction patterns of two of the three AMMs that contain presolar silicate/oxide grains (T98H5 and T98G8), as well as the pattern for AMM T00IBa030, which contains no presolar silicate/oxide grains, but does contain a possible SiC grain. The AMMs that contain presolar silicate grains are fine-grained, whereas T00IBa030 has a more massive compact structure. T98H5 (Fig. 5a) is dominated by low-Ca clinopyroxene with minor amounts of magnetite and goethite, both of which are secondary minerals due to the oxidation of Fe metal grains. T98G8 (Fig. 5b) contains olivine as well as pyroxene, and also contains secondary magnetite, as well as akaganéite (b-FeO(OH,Cl)). The AMM in which no presolar silicate grains were found, T00IBa030 (Fig. 5c), consists largely of olivine and low-Ca pyroxene with secondary magnetite. However, the diffraction pattern also shows the presence of magnesiowüstite (Fig. 5c) in this AMM. This mineral is thought to form through the decomposition of carbonates and phyllosilicates at low oxygen fugacity (Nakamura et al. 2001). Finally, the third

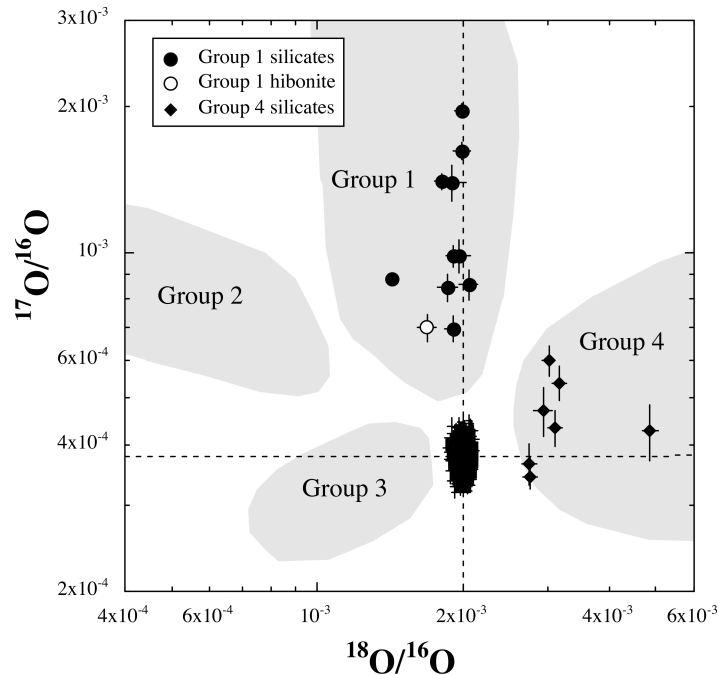


Fig. 1. Oxygen three-isotope plot showing the compositions of presolar silicates and one hibonite grain from Antarctic micrometeorites compared with isotopically normal regions from the same particles. Also shown are the classification groups for presolar oxide grains from Nittler et al. (1997). Dashed lines show solar values. Errors are  $1\sigma$ .

presolar grain-bearing AMM, TT54B397 contains low-Ca pyroxene, as well as kamacite, taenite and secondary magnetite (Nakamura, personal communication). Jarosite,  $(\text{KFe}_3(\text{SO}_4)_2(\text{OH})_6)$ , is also present in this AMM; this is a common secondary mineral that forms by alteration of sulfide minerals during their residence in the Antarctic ice (Terada et al. 2001).

## DISCUSSION

### Isotopic Compositions and Stellar Origins

The four C-anomalous grains found in this study have  $^{12}\text{C}/^{13}\text{C}$  ratios between 20 and 50. Both presolar graphite and SiC can have such ratios, but the relative distributions of C isotopic compositions in presolar graphite and SiC (e.g., Fig. 6 of Zinner 2004) suggest that the grains found here are SiC rather than graphite. Mainstream SiC grains, as well as Z grains and some X grains (see Zinner 2004 for the classification of presolar SiC) have C isotopic compositions that overlap with the range of the grains measured here. However, Si isotopic compositions can be used to distinguish among these groups. The Si isotopic compositions of most mainstream SiC grains are characterized by enrichments in the heavy isotopes of up to  $\sim 200$  ‰ and, in a three isotope Si plot, fall along a line of slope 1.4 that is shifted slightly to the right of the solar composition (e.g., Fig. 2). In contrast, SiC X grains are enriched in  $^{28}\text{Si}$  (Fig. 2), and Z grains have mostly negative  $\delta^{29}\text{Si}$  values and plot to the right of the

mainstream correlation line, typically with  $^{30}\text{Si}$  excesses relative to  $^{29}\text{Si}$  (Zinner 2004). All three carbonaceous grains that were measured for Si isotopes have isotopic compositions that are normal within errors (Table 1 and Fig. 2) and, thus, are most consistent with a mainstream SiC classification. Moreover, the N isotopic composition of one grain (T00IBa030-10P1) is also within the range of mainstream SiC grains. The isotopic signatures of mainstream SiC grains are generally consistent with an origin in carbon-rich asymptotic giant branch (AGB) stars. The  $^{13}\text{C}$  and  $^{14}\text{N}$  excesses found in mainstream grains are produced by hydrogen burning in the CNO cycle during the main sequence phase of the stars. Mixing of  $^{12}\text{C}$  produced by shell He burning during the AGB phase into the stellar envelope leads to C-rich conditions, necessary for the condensation of SiC, and produces a range of  $^{12}\text{C}/^{13}\text{C}$  ratios. The grains' Si isotopic compositions mostly reflect the initial ratios of their parent stars and are not much affected by AGB nucleosynthesis (e.g., Clayton et al. 1991; Alexander 1993; Timmes and Clayton 1996; Zinner et al. 2006a).

All of the O-anomalous grains found in the AMMs studied here belong to either group 1 or group 4. Eleven of the presolar silicate grains and the hibonite grain belong to group 1. These grains are generally thought to originate in the envelopes of oxygen-rich red giant or AGB stars that have undergone the first dredge-up (Nittler et al. 1997). Hydrogen burning in the CNO cycle in inner layers of the star during the hydrostatic phase results in the destruction of  $^{18}\text{O}$  and enhancement of  $^{17}\text{O}$  relative to the initial composition of the

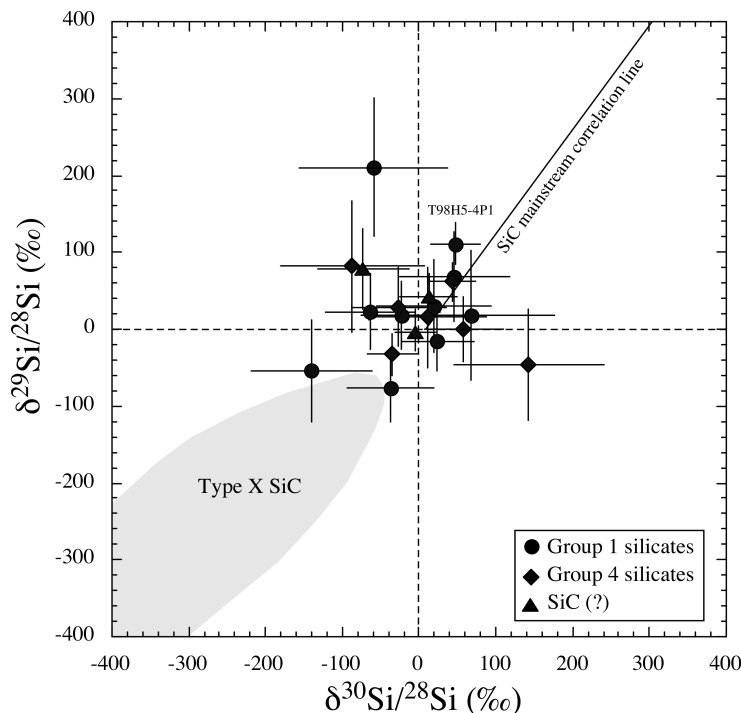


Fig. 2. Silicon three-isotope plot (expressed in per mil deviation from solar) showing the compositions of presolar silicate and (possible) SiC grains from Antarctic micrometeorites. Also shown is a portion of the range of Si isotopic compositions observed in type X SiC grains and the correlation line for mainstream SiC grains (Zinner 2004). Dashed lines show solar values. Errors are 1σ.

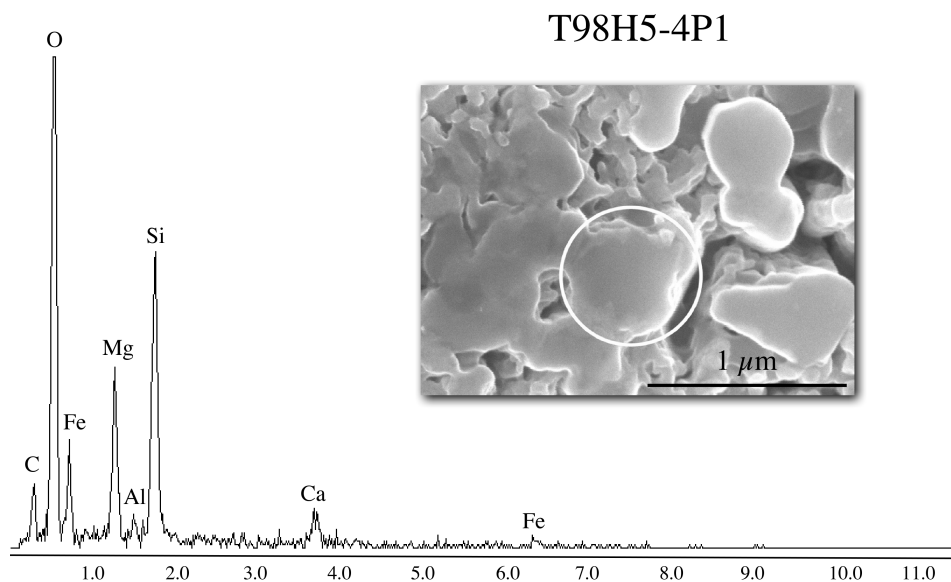


Fig. 3. Presolar grain T98H5-4P1: the EDX spectrum of the grain shown in the secondary electron image is similar to that of a Ca-rich pyroxene.

star (Boothroyd and Sackman 1999). Mixing of the  $^{17}\text{O}$ -rich and  $^{18}\text{O}$ -depleted layer during the first dredge-up to the surface of the star where grain formation occurs results in grains with enhanced  $^{17}\text{O}/^{16}\text{O}$  and somewhat depleted  $^{18}\text{O}/^{16}\text{O}$  ratios. The final  $^{17}\text{O}/^{16}\text{O}$  ratio reflects the mass of the star, whereas the final  $^{18}\text{O}/^{16}\text{O}$  ratio can be used to infer the initial

composition (i.e., metallicity) of the parent star of a given grain (Nittler et al. 1997). The group 1 presolar grains reported here all have oxygen isotopic compositions consistent with origins in low-mass ( $\leq 2.5 M_{\odot}$ ) AGB stars with a variety of initial O isotopic compositions.

The stellar sources of the seven group 4 grains are less

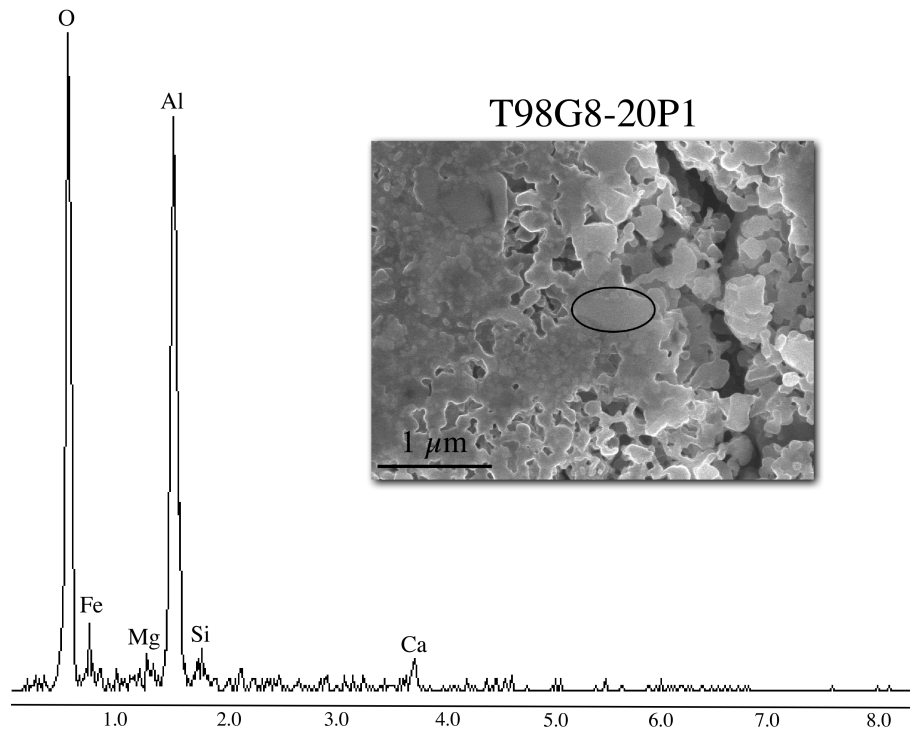


Fig. 4. Presolar grain T98G8-20P1: the EDX spectrum of the grain shown in the secondary electron image is similar to that of hibonite.

clear. Enrichments in the heavy O isotopes could indicate an origin in high-metallicity AGB stars (Nittler et al. 1997; Mostefaoui and Hoppe 2004). If the group 4 grains originate from high-metallicity AGB stars, they are expected, like group 1 grains, to exhibit enhancements in  $^{17}\text{O}$  as a result of the first dredge-up; however, all of the group 4 grains studied here have  $^{17}\text{O}/^{16}\text{O}$  ratios that are lower than expected from galactic chemical evolution (e.g., Nittler et al. 1997). Type II supernovae origins have also been suggested for some grains with large  $^{18}\text{O}$  enrichments (Choi et al. 1998; Messenger et al. 2005; Nittler et al. 2005; Zinner et al. 2006b). More recently, Nittler et al. (2008) have argued that most group 4 silicate and oxide grains have a type II supernova origin, including some for which a high-metallicity AGB origin had previously been advocated (e.g., Mostefaoui and Hoppe 2004). However, Floss et al. (2008) noted that the Fe and O isotopic compositions of a group 4 FeO grain from the Acfer 094 carbonaceous chondrite could not be reproduced by mixing of different supernova zones, and favored an AGB source for this grain.

Silicon isotopes measured to date in presolar silicate grains follow a trend similar to that observed in mainstream SiC grains, but that is shifted slightly to the left of the mainstream correlation line (Mostefaoui and Hoppe 2004; Nguyen et al. 2007). As for mainstream SiC grains, the Si isotopic compositions of presolar silicate grains primarily reflect the initial compositions of their parent stars. The presolar silicate grains from this study mostly have Si isotopic compositions that are solar within  $3\sigma$  errors (Fig. 2). The

single grain with an anomalous Si isotopic composition (T98H5-4P1) is enriched in the heavy isotopes of Si and falls near the mainstream correlation line, consistent with data from past studies (Mostefaoui and Hoppe 2004; Nguyen et al. 2007). It is interesting to note that this group 1 grain has the most  $^{18}\text{O}$ -depleted composition of all of the presolar grains from this study, with an  $^{18}\text{O}/^{16}\text{O}$  ratio of 0.0014 (Table 1). The enrichment in the heavy isotopes of Si suggests an origin in a higher than solar metallicity star, whereas the sub-solar  $^{18}\text{O}/^{16}\text{O}$  ratio of this grain would seem to indicate a low-metallicity origin. A possible explanation may be that the parent star from which this grain originated experienced cool bottom processing (e.g., Wasserburg et al. 1995; Nollett et al. 2003), during which slow circulation of material from the star's envelope through hot regions near the H shell results in decreased  $^{18}\text{O}/^{16}\text{O}$  ratios relative to the initial composition of the parent star. Calculations have shown that cool bottom processing can plausibly account for the O isotopic compositions (and high  $^{26}\text{Al}/^{27}\text{Al}$  ratios) of most group 2 grains (Wasserburg et al. 1995; Nollett et al. 2003). Moreover, Nittler et al. (2008) note that some group 1 grains, specifically those with  $^{18}\text{O}/^{16}\text{O}$  ratios of  $<0.0015$ , may also have been affected by cool bottom processing. Thus, grain T98H5-4P1 may have originated from a parent star with a somewhat higher metallicity than that indicated by its oxygen isotopic composition.

The Si isotopic compositions of the group 4 grains discussed above may provide some constraints on the origin of these grains. If these grains originate from high-metallicity

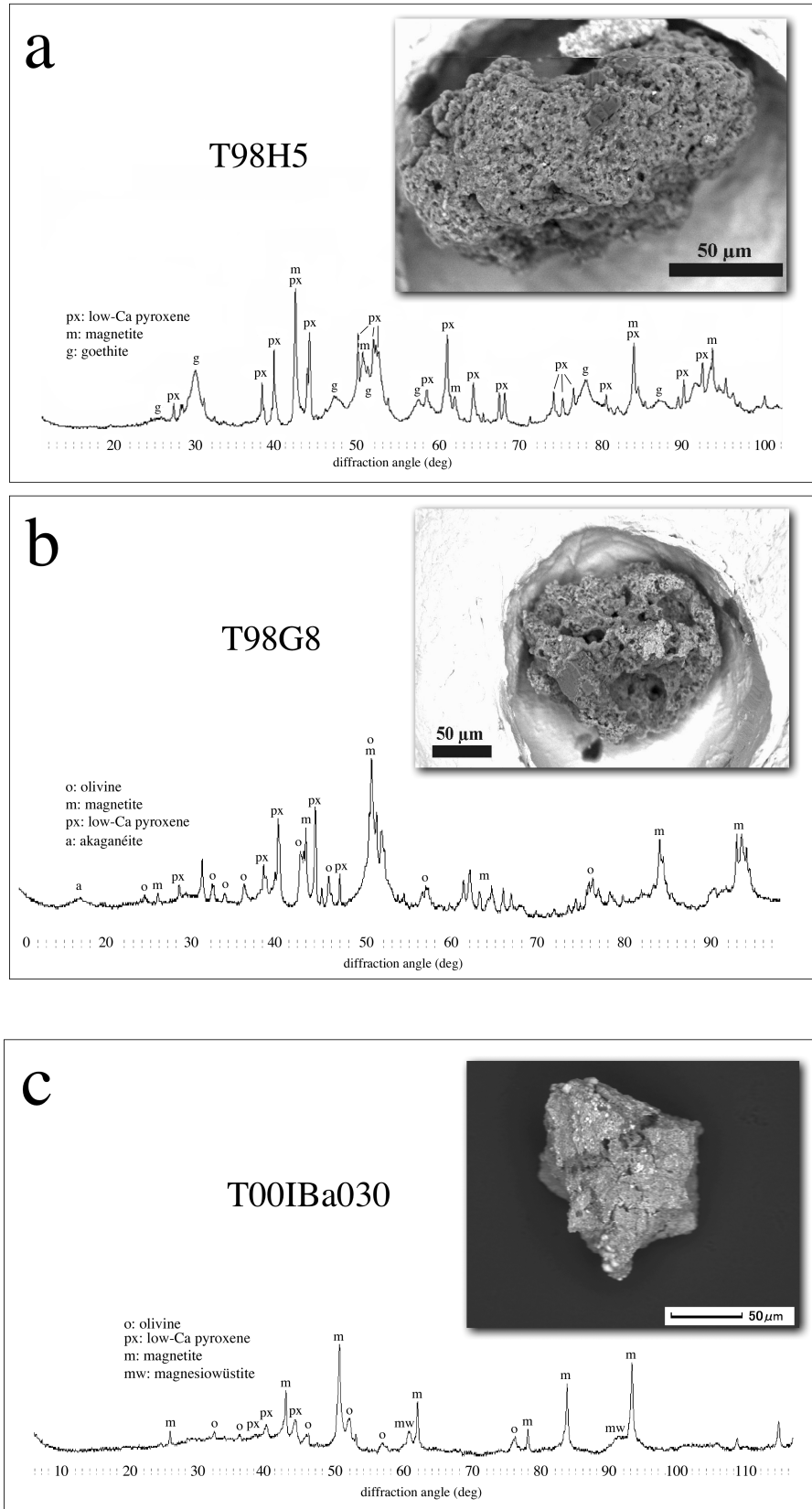


Fig. 5. Backscattered electron images and X-ray diffraction spectra for Antarctic micrometeorites: a) T98H5, b) T98G8, and c) T00IBa030.

stars, one would expect them to have heavy Si isotopic compositions (Timmes and Clayton 1996). However, the Si isotopic compositions of all of the group 4 grains are indistinguishable from those of the group 1 grains. This, combined with the lower than expected  $^{17}\text{O}$  enrichments (see above), may argue against an AGB origin for these grains from the AMMs. However, a supernova origin is also problematical. Consideration of the  $15 M_{\odot}$  supernova model of Rauscher et al. (2002) shows that condensation of grains with essentially normal Si isotopic composition can only be accomplished with material from the outermost layers (He/N zone and H envelope). These layers, however, cannot be mixed in any way to reproduce the O isotopic compositions of most group 4 grains without a small contribution from the O-rich inner layers, which would lead to significant Si isotopic anomalies. Overall a supernova origin for these grains may be more likely, because it provides a mechanism for  $^{18}\text{O}$  enrichments. However, presolar grains from group 4 may have more than one type of stellar source and probably need to be considered individually; in many cases isotopic compositions from additional elements may be required to assign a specific source.

### Distribution of O-Anomalous Grain Groups in Extraterrestrial Materials

It has been noted that the oxygen isotopic distributions of presolar silicate grains in IDPs (Messenger et al. 2003; Floss et al. 2006) and presolar silicate/oxide grains in primitive carbonaceous chondrites (Nguyen et al. 2007) differ from the distribution of presolar oxide grains from earlier studies (Nittler et al. 1997, 2005; Choi et al. 1998, 1999; Zinner et al. 2003, 2005). Specifically, group 1 and 4 grains appear to be more common among the former, whereas group 2 grains are found more often in the latter. This appears to be true as well for the AMMs studied here, as all grains observed belong to either group 1 or group 4. However, Nguyen et al. (2007) have noted that the scarcity of group 2 grains among presolar silicates/oxides is likely a consequence of the different analysis methods used to locate the grains. Nittler et al. (1997) used low mass resolution ion imaging of  $^{18}\text{O}/^{16}\text{O}$  ratios to locate many presolar oxide grains from an acid residue of Tieschitz; this method creates a bias against grains with normal  $^{18}\text{O}/^{16}\text{O}$  but anomalous  $^{17}\text{O}/^{16}\text{O}$  ratios, such as many of the group 1 grains. However, group 2 (and group 4) grains with anomalous  $^{18}\text{O}/^{16}\text{O}$  ratios are preferentially identified. In contrast, the raster ion imaging approach used here on AMMs (and by Nguyen et al. 2007 on tightly packed grain size separates) will result in a lower detection efficiency of grains with  $^{18}\text{O}$  (and  $^{17}\text{O}$ ) depleted compositions, due to dilution of the secondary ion signal as a result of beam overlap onto adjacent isotopically normal grains (see Nguyen et al. 2007 for a detailed discussion of this effect). Therefore, with this analytical method, grains with enrichments in  $^{17}\text{O}$  and  $^{18}\text{O}$ ,

such as group 1 and group 4 grains, are preferentially identified and group 2 grains with depletions in  $^{18}\text{O}$  and enrichments in  $^{17}\text{O}$  may be misidentified as group 1 grains.

In addition to the differences discussed above, one interesting observation of the O anomalous grains from the AMMs studied here is the relatively high abundance (37%) of group 4 grains. This is significantly higher than the relative proportion of group 4 silicate and oxide grains found to date in primitive meteorites (~9% for all grains and ~11% for grains identified by raster ion imaging; Presolar Grain Database 2007), but is similar to the abundance (33%) of group 4 grains observed in interplanetary dust particles (Messenger et al. 2003, 2005; Floss et al. 2006; Stadermann et al. 2006). In contrast, the abundance of group 4 grains appears to be unusually low in the primitive CR chondrite, QUE 99177, in which just one out of 33 O anomalous grains (3%) belongs to this group (Floss and Stadermann 2007). The significance of these differences is currently limited by the relatively low numbers of grains that have been found in the various extraterrestrial samples. Nevertheless, the results suggest a heterogeneity in the distribution of presolar silicate/oxide grain types among different types of primitive materials. One possible origin for such a heterogeneity was suggested by L. Nittler (personal communication), who noted that if most group 4 grains do indeed come from supernovae and possibly even a single supernova (as argued by Nittler 2007), these grains could have been injected into the early solar nebula, with the result that parent bodies forming in different parts of the nebula (or at different times) may have incorporated different proportions of these grains. Similar scenarios have been suggested to account for the occurrence of certain short-lived radionuclides in early solar system materials, such as the presence of  $^{26}\text{Al}$  in most Ca-Al-rich inclusions, but its absence from refractory minerals and inclusions bearing relict nuclear anomalies (e.g., Sahijpal and Goswami 1998). Clearly additional data are needed to verify the statistical significance of the abundance differences discussed above and also to establish whether most group 4 grains do indeed have a supernova origin.

### Abundances of Presolar Grains in AMMs

We calculated the abundance of presolar grains in the fine-grained AMMs studied here based on the cross-sectional areas of the grains and the total area analyzed. Errors were calculated based on counting statistics using  $1\sigma$  confidence intervals for small numbers (Gehrels 1986); Nguyen et al. (2007) provide a detailed discussion of other errors relevant to an accurate determination of presolar grain abundances. The overall abundance of presolar silicates in our AMMs is  $53^{+16}_{-12}$  ppm and of oxides (i.e., the hibonite grain) is  $4^{+9}_{-3}$  ppm. The abundance of all C-anomalous phases (presumably SiC, see above) is  $14^{+11}_{-7}$  ppm. These abundances are lower limits, as we have not made any corrections for instrumental

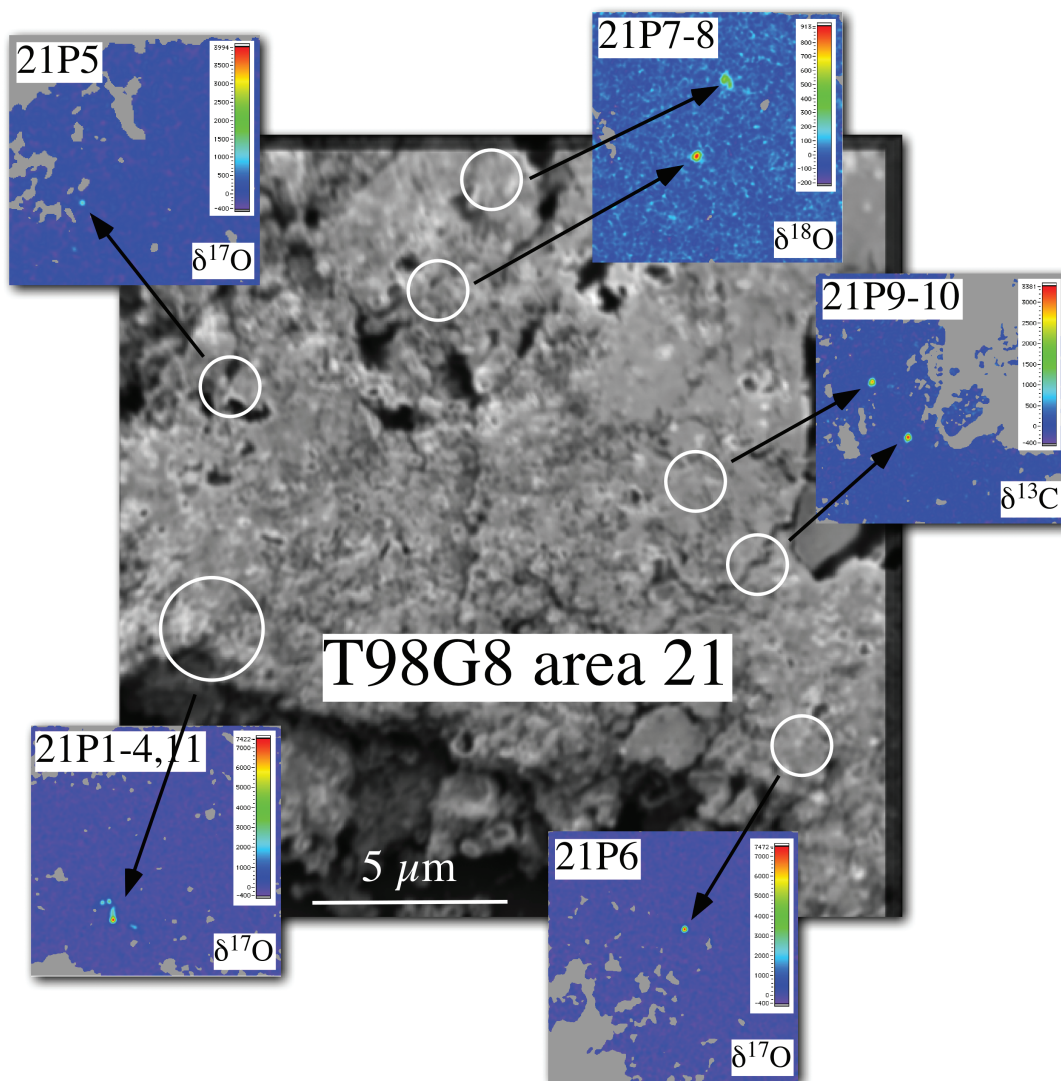


Fig. 6. NanoSIMS secondary electron image of area 21 in micrometeorite T98G8. Insets show  $\delta^{17}\text{O}$ ,  $\delta^{18}\text{O}$  or  $\delta^{13}\text{C}$  images of the 11 presolar grains found in this region of the sample. Gray areas in the  $\delta$ -value images are voids or regions where the secondary ion signals are too low for construction of meaningful isotopic ratios.

detection efficiencies (e.g., Nguyen et al. 2007). The abundance of presolar silicates in the AMMs overlaps, within errors, with the uncorrected abundances of presolar silicates in Acfer 094 and ALHA77307 ( $90 \pm 35$  and  $95 \pm 40$  ppm, respectively) determined by Nguyen et al. (2007), but the abundance of oxide grains in AMMs appears to be lower than in these meteorites ( $55 \pm 20$  and  $30 \pm 20$  ppm, respectively). The abundance of C-anomalous phases in the AMMs is similar to abundance estimates (up to  $\sim 30$  ppm) of presolar SiC in primitive carbonaceous chondrites (e.g., Gao et al. 1996; Huss et al. 2003; Zinner 2004). In contrast, isotopically primitive IDPs have a presolar silicate abundance of  $\sim 375$  ppm (not corrected for detection efficiencies; Floss et al. 2006), significantly higher than the abundances in either AMMs or primitive carbonaceous chondrites. However, abundances of C-anomalous grains in IDPs appear

to be low; although an accurate abundance estimate has not been determined, we note that, to date, only one SiC grain has been found in an IDP (Stadermann et al. 2006) and only two C-anomalous grains were found in the fourteen isotopically primitive IDPs studied by Floss et al. (2006).

The distribution of presolar grains in the AMMs studied here is, however, extremely heterogeneous. Presolar grains were only found in 4 of the 7 AMMs studied. Moreover, of the 18 presolar silicate grains found, 14 occur in one micrometeorite, T98G8, and 9 were, in fact, found in a single  $20 \times 20 \mu\text{m}^2$  area (Fig. 6). This micrometeorite also contains 3 of the 4 C-anomalous grains that were found in this study, two of which occur in the same presolar-silicate-rich region noted above (Fig. 6). If we calculate the abundances of presolar grains in this AMM (in which a total area of  $664 \mu\text{m}^2$  was analyzed), we obtain an abundance of  $170^{+58}_{-33}$  ppm for

presolar silicates and  $50_{-27}^{+48}$  ppm for C-anomalous grains. The presolar silicate abundance, at  $650_{-420}^{+840}$  ppm, is even higher in TT54B397 but, as is evident from the large uncertainty, this value is very uncertain due to the fact that only two grains were found and a relatively small total area was analyzed ( $\sim 525 \mu\text{m}^2$ ).

Presolar silicate grains in IDPs predominantly occur in an isotopically primitive sub-group of these particles. These IDPs are characterized by the presence of anomalous bulk N isotopic compositions and abundant  $^{15}\text{N}$ -enriched hotspots (Floss et al. 2006). Although isotopically primitive IDPs have not yet been definitively linked to a particular class of meteorites or parent body (including comets), it is likely that such an association exists. For example, CR chondrites are characterized by bulk  $^{15}\text{N}$  enrichments similar to those seen in these IDPs (e.g., Floss and Stadermann 2005; Busemann et al. 2006). Although presolar silicate/oxide abundances are low in some CR chondrites, probably due to the aqueous alteration these meteorites have experienced (Nagashima et al. 2004; Floss and Stadermann 2005), recent measurements of the CR chondrite QUE 99177, which is less altered, show high abundances ( $\sim 220$  ppm) of O-rich presolar grains (Floss and Stadermann 2007). However, unlike the IDPs, this meteorite also contains very high abundances ( $\sim 145$  ppm) of C-anomalous presolar grains. Antarctic micrometeorites also sample a variety of parent bodies (Kurat et al. 1994; Engrand and Maurette 1998), and the striking differences in presolar grain abundances observed in the AMMs studied here most probably reflect differences in the parent bodies from which the AMMs originated. As discussed below, the bulk mineralogies of the micrometeorites determined by X-ray diffraction suggest that this is, indeed, the case.

### Effects of Thermal and Aqueous Alteration on Presolar Grains in AMMs

The three AMMs that contain presolar silicates consist of fine-grained assemblages of olivine, pyroxene and metal, as well as secondary magnetite and/or jarosite thought to form in the upper atmosphere and in Antarctic blue ice through oxidation and alteration of metal and sulfides (Nakamura et al. 2001). Notably, they do not contain magnesiowüstite, a secondary mineral that appears to form upon heating through the decomposition of phyllosilicates and carbonates (Nozaki et al. 2006). Magnesiowüstite is, however, present in T001Ba030 shown in Fig. 5c, as well as in two of the AMMs studied here in which no presolar grains were found (T98H3 and T98G6). Magnesiowüstite-bearing AMMs probably originated from hydrous parent bodies such as the parent bodies of carbonaceous chondrites, which commonly contain phyllosilicates and carbonates. Indeed, the formation of magnesiowüstite has been reproduced experimentally by brief heating of the matrices of hydrous carbonaceous chondrites (Nozaki et al. 2006). These authors showed that

heating of matrix material from Tagish Lake, Murchison and Orgueil resulted in the decomposition of phyllosilicates and carbonates to form magnesiowüstite and amorphous silicates at temperatures starting at 600 to 700 °C; at higher temperatures the amorphous silicates recrystallize to form secondary olivine and low-Ca pyroxene. T001Ba030 also contains magnetite framboids, seen in the upper left and bottom of its BSE image (Fig. 5c). Magnetite framboids are often observed in the hydrated matrices of carbonaceous chondrites (Brearley and Jones 1998); thus, this feature provides additional evidence that T001Ba030 was originally composed of aqueous minerals. The lack of presolar silicate grains in these magnesiowüstite-bearing micrometeorites could be the result either of the aqueous alteration experienced on their original parent bodies, which is likely to alter labile presolar silicates or re-equilibrate their oxygen isotopic compositions (e.g., Floss and Stadermann 2005), or could be due to the high temperatures they experienced during atmospheric entry heating, which may have recrystallized or destroyed such grains. However, the high temperature experienced by micrometeorites during atmospheric entry does not last long, usually less than 10 seconds (Love and Brownlee 1994). We calculated the diffusion distance of oxygen in olivine at 700 °C and at the magnetite-wüstite oxygen buffer for 10 seconds, using the oxygen diffusion rate given by Ryerson et al. (1989). The results suggest a diffusion distance of only  $2 \times 10^{-8} \mu\text{m}$ , which is smaller than the atomic diameter of oxygen. Thus, the lack of presolar silicate grains in these micrometeorites must be a result of processing on the parent bodies from which these AMMs originated.

The lack of magnesiowüstite in the three AMMs that contain presolar silicates, T98H5, T98G8 and TT54B397, suggests that these micrometeorites did not experience phyllosilicate/carbonate decomposition, but rather were originally composed primarily of anhydrous phases. In addition, the sharp reflections of low-Ca pyroxene from all three AMMs (Fig. 5; Nakamura, personal communication) indicates that the pyroxene is a primary phase, and not a phyllosilicate decomposition product; secondary olivine and pyroxene tend to have broader reflections indicative of a lower degree of crystallinity (Nozaki et al. 2006). These micrometeorites may be related to anhydrous IDPs or to primitive chondrites such as Acfer 094 or ALHA77307, which have not been thermally or aqueously altered. Nitrogen isotopic data could provide additional evidence for links to isotopically primitive IDPs or to CR chondrites that have experienced little alteration (such as QUE 99177); however, N isotopic compositions have not been measured in these AMMs.

*Acknowledgments*—We thank the Antarctic Meteorite Research Center, National Institute of Polar Research, Japan for providing the unprocessed fine-grained samples from

which the AMMs used in this study were extracted. We are grateful to Dr. Daisuke Nakashima for collecting some of the AMMs studied here. We appreciate the efforts of the undergraduate students in T. Noguchi's laboratory in collecting ~3000 AMMs from these samples. We also thank Tim Smolar for maintenance of the NanoSIMS instrument. This paper benefited greatly from careful and constructive reviews by Larry Nittler and Matthew Genge and we appreciate their comments. A portion of the research described in this paper was performed in the Environmental Molecular Sciences Laboratory, a national scientific user facility sponsored by the Department of Energy's Office of Biological and Environmental Research, and located at Pacific Northwest National Laboratory. This study was partially supported by the Research Fellowships of the Japan Society for the Promotion of Science for Young Scientists to T. Yada, and by NASA grants NNG04GG49G and NNX07AI45G to C. Floss.

*Editorial Handling*—Dr. Ian Lyon

## REFERENCES

- Alexander C. M. O'D. 1993. Presolar SiC in chondrites: How variable and how many sources? *Geochimica et Cosmochimica Acta* 57:2869–2888.
- Boothroyd A. I. and Sackmann I. J. 1999. The CNO isotopes: Deep circulation in red giants and first and second dredge-up. *The Astrophysical Journal* 510:232–250.
- Brealey A. and Jones R. H. 1998. Chondritic meteorites. In *Planetary materials*, edited by Papike J. J. Washington, D.C.: The Mineralogical Society of America. pp.3-1–3-398.
- Busemann H., Young A. F., Alexander C. M. O'D., Hoppe P., Mukhopadhyay S., and Nittler L. R. 2006. Interstellar chemistry recorded in organic matter from primitive meteorites. *Science* 312:727–730.
- Choi B.-G., Huss G., Wasserburg G., and Gallino R. 1998. Presolar corundum and spinel in ordinary chondrites: Origins from AGB stars and a supernova. *Science* 282:1284–1289.
- Choi B.-G., Wasserburg G. J., and Huss G. R. 1999. Circumstellar hibonite and corundum and nucleosynthesis in asymptotic giant branch stars. *The Astrophysical Journal* 522:L133–L136.
- Clayton D. D., Obradovic M., Guha S., and Brown L. E. 1991. Silicon and titanium isotopes in SiC from AGB stars (abstract). 22nd Lunar and Planetary Science Conference. pp. 221–222.
- Demyk A., Dartois E., Wiesemeyer H., Jones A. P., and d'Hendecourt L. 2000. Structure and chemical composition of the silicate dust around OH/IR stars. *Astronomy and Astrophysics* 364:170–178.
- Engrand C. and Maurette M. 1998. Carbonaceous micrometeorites from Antarctica. *Meteoritics & Planetary Science* 33:565–580.
- Floss C. and Stadermann F. J. 2005. Presolar (circumstellar and interstellar) phases in Renazzo: The effects of parent body processing (abstract #1390). 36th Lunar and Planetary Science Conference. CD-ROM.
- Floss C. and Stadermann F. J. 2007. Very high presolar grain abundances in the CR chondrite QUE 99177 (abstract). *Meteoritics & Planetary Science* 42:A48.
- Floss C., Stadermann F. J., Bradley J. P., Dai Z. R., Bajt S., Graham G., and Lea A. S. 2006. Identification of isotopically primitive interplanetary dust particles: A NanoSIMS isotopic imaging study. *Geochimica et Cosmochimica Acta* 70:2371–2399.
- Floss C., Stadermann F. J., and Bose M. 2008. Circumstellar Fe oxide from the Acfer 094 carbonaceous chondrite. *The Astrophysical Journal* 672:1266–1271.
- Gao X., Amari S., Messenger S., Nittler L. R., Swan P., and Walker R. M. 1996. Survey of circumstellar grains in the unique carbonaceous chondrite Acfer 094 (abstract). *Meteoritics & Planetary Science* 31:A48.
- Gehrels N. 1986. Confidence limits for small numbers of events in astrophysical data. *The Astrophysical Journal* 303:336–346.
- Huss G., Meshik A. P., Smith J. B., and Hohenberg C. 2003. Presolar diamond, silicon carbide, and graphite in carbonaceous chondrites: Implications for thermal processing in the solar nebula. *Geochimica et Cosmochimica Acta* 67:4823–4848.
- Iwata N. and Imae N. 2002. Antarctic micrometeorite collection at a bare ice region near Syowa Station by JARE-41 in 2000. *Antarctic Meteorite Research* 15:25–37.
- Kurat G., Koeberl C., Presper T., Brandstätter F., and Maurette M. 1994. Petrology and geochemistry of Antarctic micrometeorites. *Geochimica et Cosmochimica Acta* 58:3879–3904.
- Love S. G. and Brownlee D. E. 1993. A direct measurement of the terrestrial mass accretion rate of cosmic dust. *Science* 262:550–553.
- Love S. G. and Brownlee D. E. 1994. Peak atmospheric entry temperatures of micrometeorites. *Meteoritics* 29:69–70.
- Maurette M. 2006. *Micrometeorites and the mysteries of our origins*. Springer-Verlag, Heidelberg. 330 p.
- Maurette M., Hammer C., Reeh N., Brownlee D. E., and Thomsen H. H. 1986. Placers of cosmic dust in the blue ice lakes of Greenland. *Science* 233:869–872.
- Maurette M., Olinger C. T., Christophe Michel-Levy M., Kurat G., Pourchet M., Brandstätter F., and Bourot-Denise M. 1991. A collection of diverse micrometeorites recovered from 100 tonnes of Antarctic blue ice. *Nature* 351:44–47.
- Messenger S., Keller L. P., Stadermann F. J., Walker R. M., and Zinner E. 2003. Samples of stars beyond the solar system: Silicate grains in interplanetary dust. *Science* 300:105–108.
- Messenger S., Keller L. P., and Lauretta D. S. 2005. Supernova olivine from cometary dust. *Science* 309:737–741.
- Mostefaoui S. and Hoppe P. 2004. Discovery of abundant in situ silicate and spinel grains from red giant stars in a primitive meteorite. *The Astrophysical Journal* 613:L149–L152.
- Nagashima K., Krot A. N., and Yurimoto H. 2004. Stardust silicates from primitive meteorites. *Nature* 428:921–924.
- Nakamura T., Noguchi T., Yada T., Nakamura Y., and Takaoka N. 2001. Bulk mineralogy of individual micrometeorites determined by X-ray diffraction analysis and transmission electron microscopy. *Geochimica et Cosmochimica Acta* 65:4385–4397.
- Nguyen A. N. and Zinner E. 2004. Discovery of ancient silicate stardust in a meteorite. *Science* 303:1496–1499.
- Nguyen A. N., Stadermann F. J., Zinner E., Stroud R. M., Alexander C. M. O'D., and Nittler L. R. 2007. Characterization of presolar silicate and oxide grains in primitive carbonaceous chondrites. *The Astrophysical Journal* 656:1223–1240.
- Nittler L. R. 2007. Presolar grain evidence for low-mass supernova injection into the solar nebula (abstract). Workshop on the Chronology of Meteorites and the Early Solar System. pp.125–126.
- Nittler L. R., Alexander C. M. O'D., Gao X., Walker R. M., and Zinner E. 1997. Stellar sapphires: the properties and origins of presolar Al<sub>2</sub>O<sub>3</sub> in meteorites. *The Astrophysical Journal* 483:475–495.
- Nittler L. R., Alexander C. M. O'D., Stadermann F. J., and Zinner

- E. K. 2005. Presolar Al-, Ca-, and Ti-rich oxide grains in the Krymka meteorite (abstract #2200). 36th Lunar and Planetary Science Conference. CD-ROM.
- Nittler L. R., Alexander C. M. O'D., Gallino R., Hoppe P., Nguyen A. N., Stadermann F. J., and Zinner E. K. 2008. Aluminum-, calcium- and titanium-rich oxide stardust in ordinary chondrite meteorites. *The Astrophysical Journal* 682:1450–1478.
- Noguchi T., Nakamura T., and Nozaki W. 2002. Mineralogy of phyllosilicate-rich micrometeorites and comparison with Tagish Lake and Sayama meteorites. *Earth and Planetary Science Letters* 202:229–246.
- Nollett K. M., Busso M., and Wasserburg G. J. 2003. Cool bottom processes on the thermally pulsing asymptotic giant branch and the isotopic composition of circumstellar dust grains. *The Astrophysical Journal* 582:1036–1058.
- Nozaki W., Nakamura T., and Noguchi T. 2006. Bulk mineralogical changes of hydrous micrometeorites during heating in the upper atmosphere at temperatures below 1000 °C. *Meteoritics & Planetary Science* 41:1095–1114.
- Presolar Grain Database. 2007. <http://presolar.wustl.edu/~pgd>, edited by F. Gyngard.
- Prombo C. A., Nichols R. H., Alexander C. M. O'D., Swan P. D., Walker R. M., and Maurette M. 1991. SiC in Greenland lake sediments (abstract). 22nd Lunar and Planetary Science Conference. pp 1103–1104.
- Rauscher T., Heger A., Hoffman R. D., and Woosley S. E. 2002. Nucleosynthesis in massive stars with improved nuclear and stellar physics. *The Astrophysical Journal* 576:323–348.
- Ryerson, F. J., Durham W. B., Cherniak D. J., and Lanford W. A. 1989. Oxygen diffusion in olivine: Effects of oxygen fugacity and implications for creep. *Journal Geophysical Research* 94: 4105–4118.
- Sahijpahl S. and Goswami J. N. 1998. Refractory phases in primitive meteorites devoid of <sup>26</sup>Al and <sup>41</sup>Ca: Representative samples of first solar system solids? *The Astrophysical Journal* 509:L37–L40.
- Slodzian G., Hillion F., Stadermann F. J., and Zinner E. 2004. QSA influences on isotopic ratio measurements. *Applied Surface Science* 231–232:874–877.
- Stadermann F. J., Croat T. K., Bernatowicz T., Amari S., Messenger S., Walker R. M., and Zinner E. 2005. Supernova graphite in the NanoSIMS: Carbon, oxygen and titanium isotopic compositions of a spherule and its TiC sub-components. *Geochimica et Cosmochimica Acta* 69:177–188.
- Stadermann F. J., Floss C., and Wopenka B. 2006. Circumstellar aluminum oxide and silicon carbide in interplanetary dust particles. *Geochimica et Cosmochimica Acta* 70:6168–6179.
- Strebel R., Hoppe P., Eberhardt P., and Maurette M. 1998. Search for presolar silicon carbide in micrometeoritic material in a cryoconite sample from Greenland ice (abstract). *Meteoritics & Planetary Science* 33:A151.
- Taylor S., Lever J. H., and Harvey R. P. 1998. Accretion rate of cosmic spherules measured at the South Pole. *Nature* 392:899–903.
- Terada K., Yada T., Kojima H., Noguchi T., Nakamura T., Murakami T., Yano H., Nozaki W., Nakamura Y., Matsumoto N., Kamata J., Mori T., Nakai I., Sasaki M., Itabashi M., Setoyangi T., Nagao K., Osawa T., Hiyagon H., Mizutani S., Fukuoka T., Nogami K., Ohmori R., and Ohashi H. 2001. General characterization of Antarctic micrometeorites collected by the 39th Japanese Antarctic Research Expedition: Consortium studies of JARE AMMs (III). *Antarctic Meteorite Research* 14:89–107.
- Timmes F. X. and Clayton D. D. 1996. Galactic evolution of silicon isotopes: Application to presolar SiC grains from meteorites. *The Astrophysical Journal* 472:723–741.
- Wasserburg G. J., Boothroyd A. I., and Sackmann I. J. 1995. Deep circulation in red giant stars: A solution to the carbon and oxygen isotope puzzles? *The Astrophysical Journal* 447:L37–L40.
- Waters L. B. F. M., Molster F. J., de Jong T., Beintema D. A., Waelkens C., Boogert A. C. A., Boxhoorn D. R., de Graauw T., Drapatz S., H. F., Genzel R., Helmich F. P., Heras A. M., Huygen R., Izumiura H., Justtanont K., Kester D. J. M., Kunze D., Lahuis F., Lamers H. J. G. L. M., Leech K. J., Loup C., Lutz D., Morris P. W., Price S. D., Roelfsema P. R., Salama A., Schaeidt S. G., Tielens A. G. G. M., Trams N. R., Valentijn E. A., Vandenbussche B., van den Ancker M. E., van Dishoeck E. F., van Winckel H., Wesselius P. R., and Young E. T. 1996. Mineralogy of oxygen-rich dust shells. *Astronomy and Astrophysics* 315:L361–L364.
- Yada T. and Kojima H. 2000. The collection of micrometeorites in the Yamato meteorite ice field of Antarctica in 1998. *Antarctic Meteorite Research* 13:9–18.
- Yada T., Nakamura T., Takaoka N., Noguchi T., Terada K., Yano H., Nakazawa T., and Kojima H. 2004. The global accretion rate of extraterrestrial materials in the last glacial period estimated from the abundance of micrometeorites in Antarctic glacier ice. *Earth Planets and Space* 56:67–79.
- Yada T., Stadermann F. J., Floss C., Zinner E., Olinger C. T., Graham G. A., Bradley J. P., Dai Z. R., Nakamura T., Noguchi T., and Bernas M. 2005a. Discovery of abundant presolar silicates in subgroups of Antarctic micrometeorites (abstract #1227). 36th Lunar and Planetary Science Conference. CD-ROM.
- Yada T., Stadermann F. J., Floss C., Zinner E., Olinger C. T., Graham G. A., Bradley J. P., Dai Z. R., Nakamura T., and Noguchi T. 2005b. The stellar origins of presolar silicates discovered in Antarctic micrometeorites (abstract). 30th NIPR Symposium on Antarctic Meteorites. pp 94–95.
- Yada T., Stadermann F. J., Floss C., Zinner E., Nakamura T., Noguchi T., and Lea A. S. 2006. High abundances of presolar silicates in Antarctic micrometeorites; implications for their cometary origins (abstract #1470). 37th Lunar and Planetary Science Conference. CD-ROM.
- Yates P. D. 1993. Micrometeorite presolar diamonds from Greenland cryoconite (abstract)? 24th Lunar and Planetary Science Conference. pp 1559–1560.
- Zinner E. 2004. Presolar grains. In *Meteorites, planets and comets*, edited by Davis A. M. Treatise on Geochemistry, vol. 1. Amsterdam: Elsevier. pp. 17–39.
- Zinner E., Amari S., Guinness R., Nguyen A., Stadermann F., Walker R. M., and Lewis R. S. 2003. Presolar spinel grains from the Murray and Murchison carbonaceous chondrites. *Geochimica et Cosmochimica Acta* 67:5083–5095.
- Zinner E., Nittler L. R., Hoppe P., Gallino R., Straniero O., and Alexander C. M. O'D. 2005. Oxygen, magnesium and chromium isotopic ratios of presolar spinel grains. *Geochimica et Cosmochimica Acta* 69:4149–4165.
- Zinner E., Nittler L. R., Gallino R., Karakas A. I., Lugaro M., Straniero O., and Lattanzio J. C. 2006a. Silicon and carbon isotopic ratios in AGB stars: SiC grain data, models, and the Galactic evolution of the Si isotopes. *The Astrophysical Journal* 650:350–373.
- Zinner E., Nittler L. R., Alexander C. M. O'D., and Gallino R. 2006b. The study of radioisotopes in presolar dust grains. *New Astronomy Review* 50:574–577.